Solidification of Precirol (R) by the expansion of a supercritical fluid saturated melt: From the thermodynamic balance towards the crystallization aspect

Marilyn Calderone, Élisabeth Rodier, Jean-jacques Letourneau, Jacques Fages

Solidification of Precirol® by the expansion of a supercritical fluid saturated melt: From the thermodynamic balance towards the crystallization aspect

Marilyn Calderone, Elisabeth Rodier*, Jean-Jacques Letourneau, Jacques Fages

École des Mines d'Albi-Carmaux, RAPSODEE Research Centre-UMR CNRS 2392, 81013, Albi, France

Abstract

The following article presents the thermodynamic and crystallization aspects of the solidification through expansion of a melted fat, Precirol®, previously saturated with supercritical CO_2. A simplified macroscopic energy balance is used to understand the mixture behaviour during expansion. It allows the quantification of the CO_2 to be added to the mixture in order to control the state and the temperature of the compound at the outlet of the expansion device. The required physico-chemical parameters were determined experimentally. The variation of the operating parameters appearing in the energy balance revealed three regions/areas of possible states for the expanded lipid: solid, molten or solid–liquid equilibrium. This, together with the outlet temperature could be tuned by varying not just the inlet or saturation conditions, but also the ratio of supercritical CO_2 to be expanded with the saturated fat. As for the crystallization aspect, the variation of chemical potential, which is the driving force, was calculated; the critical radius of nuclei and the nucleation rates were estimated according to the classic melt media theory. The main assumptions were that solidification occurred mainly at atmospheric pressure and that only homogeneous nucleation took place. The orders of magnitude obtained put in light the necessity to determine precisely the viscosity of the melt saturated fat and the solid/melt interfacial tension.

Keywords: Supercritical fluids; Thermodynamics process; Crystallization; Particle formation; Nucleation rate; Fats

1. Introduction

Supercritical fluids and especially supercritical CO_2 are an attractive substitute of an organic solvent for the generation of micro or nanoparticles with controlled size and morphology [1–2]. Compared to classical powder generation processes they include an additional varying parameter, the pressure, which greatly influences the density of the supercritical fluid. So, the supercritical technology uses the variation of both pressure and temperature to design particle size and morphology.

Among the main principles involved in supercritical processes, one is based on the use of the supercritical fluid as a solute. For instance, the process known as PGSS^{TM}, for Particles from Gas Saturated Solutions, is based on this principle [3]. It involves the dissolution of a dense gas into a liquid or a molten solid until its saturation. This saturated compound is then expanded through a nozzle where the cooling due to the pressure drop generates dry powder. In a varying process both the saturated solution and the supercritical fluid are expanded [4]. These processes are easy to perform and can be applied to a large number of compounds since dense gases are quite soluble in liquids or melted solids. It has been shown to be effective for the generation of particles from various compounds such as polymers, fats, and pharmaceuticals, in addition to composite particles [5–6]. In such processes, the Joule Thomson effect caused by the expansion induces a drastic undercooling, which induces solidification of the melted compound. As the undercooling amplitude is a key-factor for crystallization mechanisms, it is necessary to model it in order to control the process. So far, the literature has not yet dug deep enough into the understanding of these particle formation processes. Elvassore et al., considered the thermodynamic aspect of PGSS^{TM} applied to pure tristearin or a 50:50 mixture of phosphatidylcholin and tristearin [7]. From the calculation of the enthalpy variation upon the expansion step, the authors determined the final temperatures that were reached. They chose to consider the expansion of a saturated solution without any excess

* Corresponding author. Tel.: +33 5 63 49 31 25; fax: +33 5 63 49 30 25.
E-mail address: rodier@enstimac.fr (E. Rodier).

Nomenclature

a	attraction parameter in Peng–Robinson equation of state (Pa m^6/mol^2)
A	cross section area (m^2)
b	van der Waals co volume (m^3/mol)
C_p	isobaric mass heat capacity (J/(kg K))
d_0	molecular diameter (m)
E_v	activation energy (J)
f_L	lipid–liquid fraction after expansion, quantity of liquid on the total lipid expanded
G	growth rate (m/s)
h	mass enthalpy (J/kg)
H	molar enthalpy (J/mol)
J	nucleation rate (nuclei/m^3/sec) or (nuclei/cm^3/s)
k	Boltzmann's constant, 1.38×10^{-23} (J/K)
K	constant of the Stephan–Shapski–Turnbull's law
m	weight (kg)
$\dot{m}$	mass flow rate (kg/s)
P	pressure (Pa)
r	solubility ratio (kg_{CO_2}/$kg_{Precirol}$)
r_c	critical radius of nuclei (m)
R	perfect constant gas 8.314 J/(kg mol)
s_k	mass entropy of the state k, J/(mol K)
S	mass ratio of dissolved CO_2 compared to the total CO_2 (kg/kg)
S_k	molar entropy of the state k (J/(kg K))
T	temperature (K)
T_F	final temperature reached by the system at the nozzle outlet (K)
T_{melt}	normal melting point (K)
u	velocity (m/s)
v_L	specific volume (m^3/kg)
v_o	molecular volume (m^3/mol)
V	volume (m^3)
w_{CO_2}	mass ratio of CO_2 into the mixture before expansion

Greek letters

α	shape factor
β	shape factor
γ	interfacial tensile strength (J/m^2)
η	dynamic viscosity (kg/(m s))
μ	driving force (J/kg)
ρ	density (kg/m^3)
ω	acentric factor
Δ	properties variation

Subscripts

atm	atmospheric pressure and temperature properties
c	critical
crist	crystallization
d	divergent diss, dissolution
F	final state at the nozzle outlet
in	inlet conditions
L	liquid phase
melt	melting properties
out	outlet conditions
S	solid phase
SC	supercritical conditions
SL	refer to solid–liquid surface tension
V	gaseous state

Superscripts

®	Registered
TM	Trade mark

CO_2 in the vessel. The macroscopic energy balance was solved, based on both experimental methods, using apparatus like differential scanning calorimetry (DSC), to measure the calorimetric parameters of the lipids, and a theoretical approach, using the perturbed hard sphere chain theory model (PHSCT) to estimate the solubility of CO_2 in the lipid. On the pressure–temperature phase diagram of the binary fat/CO_2, three different areas were distinguished, corresponding to three different final states of the fat: solid, solid/liquid equilibrium or liquid. The authors noticed that the area that led to solid nanoparticles was directly linked to the heat of solidification of the fat. In addition, the authors reported some variations between the heat of fusion and the heat of formation (or crystallization) for the pure compound processed by PGSS™ or not. The very fast crystallization of PGSS™ from a melt is responsible for the observed variations, due to the modification of the structure of the lipid. Li and Matos, did the most complete model for particle formation by PGSS™, on the hydrogenated palm oil/CO_2 system [8]. The authors considered the influence of the nozzle hydrodynamic on particle size as well as the thermodynamic and crystallization aspects. Most of the parameters required for the modelling were estimated by calculation, except calorimetric parameters that were measured via a DSC apparatus. They considered the expansion in steady state conditions of the mixture: saturated melt phase and the supercritical CO_2. The model aimed to determine the profiles of pressure, temperature, densities, volume fraction of CO_2 in the melt phase or in the whole system, as well as the mean particle diameter along the nozzle. The volume fraction of excess CO_2 that was expanded was calculated along the nozzle, and was initialized to 0.95 at the inlet, based on a their previous experiments [9]. The crystallization was considered, taking into account nucleation, condensation and coagulation of the solute and assuming a homogeneous nucleation, rather than the classical heterogeneous one, since crystallization processes using supercritical fluids are very fast, and therefore far from equilibrium conditions. The authors reached typical values for critical nucleus, particle average size and nucleation rates on the basis of assumptions from molten metal crystallization. These authors showed that the mean particle diameter depends directly on both the critical nucleus volume and nucleation rates that are drastically affected by the undercooling. From a hydrodynamic point of view, the results show that the nozzle diameter has a moderate influence on the size of the particles obtained; because coagu-

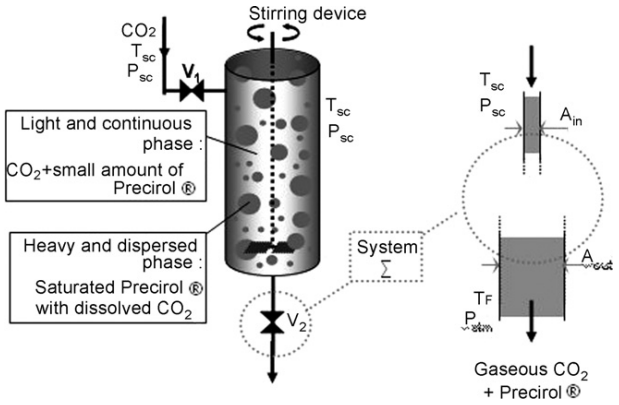

Fig. 1. Open system considered for the thermodynamic balance.

lation and condensation effects in the nozzle are limited, the authors noticed that increasing the nozzle diameter increased particle yield with only a small increase in the particle mean diameter. In agreement with Elvassore et al., the authors found evidence of limiting temperatures and pressures, above which, the expansion was led by lipid droplets or solid lipid particles [7].

From the previous papers, it appears that there are two major factors in such processes that control the final state of the particles. First, considering the thermodynamic of the process, the operating conditions, pressure and temperature, are necessary to anticipate the state of the lipid after its expansion. The second influential factor for particle size is the undercooling, that controls the nucleation rate of the compound and thus the solid particle flow rate.

In the present paper, a macroscopic energy balance of the expansion step is investigated. This allowed to quantify the effect of the CO_2 ratio (in excess or not) in the fat/CO_2 mixture, on the outlet temperature. The crystallisation in terms of driving force, critical radius of the nuclei and nucleation rate was also analysed. So, the energy balance of the expansion step of this process is established and applied to a mixture of fatty compounds. The quantity of CO_2 that is expanded is a varying parameter. The system used is CO_2/Precirol® ATO 5. A system with a heavy phase that contains melted Precirol® saturated by supercritical CO_2 and a light one that is mainly composed of supercritical CO_2 was considered. Both phases are supposed to be mixed homogeneously. In the present process, expansion cools the mixture and then the solidification of the fatty compound occurs. The crystallization is assumed to take place mostly after expansion, so it was also assumed that crystallization occurs at atmospheric pressure. Consequently, it is supposed that the implied crystallization mechanisms are similar to those implied in classical melt media theory and that the nucleation is homogeneous.

1.1. Definition of the system and assumptions

Fig. 1 presents the open system Σ considered. Before expansion, the vessel contains a stirred mixture of a light and a heavy phase. The temperature (T_{SC}) and the pressure (P_{SC}) are above the critical coordinates of the CO_2. The light phase is mainly composed of supercritical CO_2 with a small amount of extracted Precirol® (at the detection limit). The heavy phase is a mixture of melted Precirol® saturated by supercritical CO_2. From now on, the expression liquid for the melted Precirol will be used, whatever the saturation level with CO_2. For instance, at 11 MPa and 323 K, 0.31 g of CO_2 is dissolved per gram of Precirol® [10]. The valve V_2 is open and the mixture expands through the system Σ. During the transformation the valve V_1 is still opened in order to keep a constant pressure P_{SC} into the vessel. After expansion, the two components are completely separated, the outlet temperature is T_F and the outlet pressure (P_{atm}) is atmospheric.

Table 1
CO_2 critical parameters and acentric factor to solve P.R. EoS

CO_2 parameter	P_c (MPa)	T_c(K)	ω
Values	7.38	304.2	0.225

The open system Σ shown in the Fig. 1 is supposed to be in steady state. Other assumptions are:

- The transformation is considered to be adiabatic.
- The overall time, during which the valve V_2 is open, is short enough and, the volume of the vessel is big enough, to consider that the composition of the mixture into the vessel does not change during the transformation. Furthermore, this mixture is supposed to be stirred so as to obtain a homogeneous composition of the flow downstream the vessel.
- Both components are totally separated after expansion; CO_2 becomes gaseous, without becoming solid. This last assumption is justified by in situ experimental temperature measurements at the expansion device outlet. Indeed, the lowest temperature measured was found at 243 K. This value is far from the CO_2 sublimation point at atmospheric pressure: 194.2 K.
- No other forces but those of pressure are taken into account; this means that any increase of internal energy by viscous dissipation is neglected.
- Melted Precirol® is supposed to behave as an incompressible fluid. The reference state is for a molten compound in the initial supercritical conditions.
- The Peng–Robinson equation of state (P.R. EoS) is used to represent CO_2 behaviour [11].

  This equation was found to give good enthalpy data under supercritical conditions [12]. The used expressions can be found in Appendix A.

  The critical values and the acentric factor of CO_2 used to solve P.R. EoS are given in Table 1 [13]. The reference state chosen in the present study were the standard ones at supercritical initial temperature.
- The variation of kinetic energy of the system is supposed negligible. The demonstration of this assumption can be found in Appendix B.

Considering all these assumptions, the expansion was found to be isenthalpic:

$$\dot{m}h_{in} = \dot{m}h_{out} \quad (1)$$

This equation leads to the following relation, which is explained in Appendix C:

$$w_{CO_2}[h_{CO_2,V}(T_F, P_{atm}) - h_{CO_2,SC}(T_{SC}, P_{SC}) - S\Delta h_{diss}(T_{SC}, P_{SC})] + \ldots (1 - w_{CO_2})[(1 - f_L)\Delta h_{crist} - c_{P,L}(T_{SC} - T_{melt}) - (1 - f_L)(\Delta c_{P,melt})(T_F - T_{melt}) - v_L(P_{SC} - P_{atm})] = 0 \quad (2)$$

1.2. Investigations in terms of fat solidification: driving force, critical radius and nucleation rates

According to [14], the driving force $\Delta\mu(T_F)$ associated with the classical melt media theory can be given by:

$$\Delta\mu(T_F) = \Delta s_{melt}\Delta T - \frac{\Delta c_{P,melt}}{2T_{melt}}\Delta T^2 \quad (3)$$

This expression assumes crystallization at atmospheric pressure. The second term is generally required for complex mixtures or polymers. In this expression, ΔT is the undercooling, the difference between the normal melting point T_{melt} and the final temperature T_F reached by the expanded system. Δs_{melt} and $\Delta c_{P,melt}$ are respectively, the variation of the entropy and specific heat capacities involved during the crystallization step:

$$\Delta s_{melt} = s_L(T_{melt}) - s_s(T_{melt}) = \frac{\Delta h_{crist}}{T_{melt}} \quad (4)$$

$$\Delta c_{P,melt} = c_{P,L}(T_{melt}) - c_{P,S}(T_{melt}) \quad (5)$$

The undercooling, ΔT is linked to the critical radius r_c of the formed nuclei according to the relation:

$$r_c = \frac{2\gamma_{SL}v_0}{(\Delta H_{crist}/T_{melt})\Delta T} \times \frac{\beta}{3\alpha} \quad (6)$$

The critical radius is the limit size above, which the nucleus is stable and will grow. In (6) γ_{SL} is lipid solid/liquid tensile strength, $\beta/3\alpha$ is a shape factor, supposed to be equal to one since spherical particles were assumed, and v_0 is the molar volume.

Considering a homogeneous nucleation and sphere like particles, the nucleation rate J can be calculated knowing the undercooling [15]:

$$J = \frac{A_0}{\eta(T)} \times \exp\left(\frac{B}{T\Delta T^2}\right) \quad (7)$$

where:

$$B = \frac{16\pi v_0^2\gamma_{SL}^3}{3k\Delta S_{melt}^2} \quad (8.1)$$

$$A_0 = \frac{2(\gamma_{SL}kT)^{1/2}}{3\pi d_0^2 v_0} \times \exp\left(-\frac{\Delta S_{melt}}{k}\right) \quad (8.2)$$

$$d_0 = \left(\frac{6v_0}{\pi}\right)^{1/3} \quad (8.3)$$

In (7), $\eta(T)$ is the viscosity of the solution before crystallization. It has been observed that, for lipid or fat materials in supercritical media, the viscosity can be reduced up to 90% according to the pressure (for similar CO_2 solubilities as for Precirol®) compared to the viscosity at atmospheric pressure [16]. In (8.1) and (8.2), k is the Boltzmann's constant.

2. Materials and methods

2.1. Materials

Precirol® (Gattefosse, France) is a solid mixture of mono, di and triglycerides, mainly composed of a diglyceride of palmitic and stearic acids. Its normal melting point is 329.5 ± 0.3 K and its molar weight, according to the supplier, is 615 g/mol. Precirol® is known as safe and is largely added to pharmaceutical formulations as an excipient for controlled release applications, for example [17–18]. CO_2 (purity 99.995%) was supplied by Air Liquide (France) and used without any further purification.

2.2. Determination of calorimetric parameters: fusion temperature, heat of fusion, heat of CO_2 dissolution into the fat

The different parameters and experimental apparatus required to determine these parameters are gathered in Table 2.

A DSC 7 (Perkin-Elmer, UK) was used to determine the heat of fusion and the melting point of Precirol®. The measurement was done under nitrogen gas flow from 293 to 363 K at 5 K/min on a weighed sample of 4×10^{-3} g. The heat of fusion of supplied Precirol® was 114.3 ± 1.9 J/g. This value was supposed to be the same as the heat of crystallization. Its fusion temperature was 329.9 ± 0.5 K.

A Setaram® C80 microcalorimeter (Setaram, France) was used to find the Precirol® solid and liquid heat capacities. 3.9 g of Precirol® was placed in a closed cell and heated from 298 to 373 K at 0.5 K/min. The derivation of the heat flow according to temperature gives the heat capacity.

The microcalorimeter was also modified to measure the dissolution enthalpy of CO_2 into the fat. Our experimental set up was limited to pressures below 5 MPa. However, this experiment allowed for the approximation of the value of dissolution enthalpy. About 1.29 g of Precirol® was placed into an open high-pressure cell. First, the temperature cell was stabilized to 336.37 K in order to have Precirol® in a liquid state. The cell was simultaneously purged with CO_2 at atmospheric pressure. Then the cell was pressurized with dense CO_2 of up to 4 MPa. The time of pressurization was negligible compared to the time of heat flow measurement, which was about 75 min. The same experiment was performed without any Precirol® to obtain a blank, which was subtracted to the former experiment.

2.3. Solubility of CO_2 into Precirol® and solid/liquid/gas equilibrium

The solubility of Precirol® was determined using a static method. The method has been described elsewhere [10]. Briefly, it consists of placing about 10 g of Precirol® into a high-pressure cell, then introducing supercritical CO_2 at a pressure and temperature of interest. The binary mixture was agitated using a

Table 2
Physico-chemical parameters to calculate the thermodynamic balance

Parameters	Δh_{diss} (J/g)	$C_{P,L}$ (J/(g K))	$C_{P,S}$ (J/(g K))	v_L (m^3/g)	Δh_{crist} (J/g)	T_{melt} (K)
Determination	Calorimeter under CO_2 flow	Calorimeter	Calorimeter	Pycnometer	DSC	DSC
Values	3.1 ± 1.3	2.26	1.84	1.11×10^{-6}	−114.3	330.1

magnetic stirrer. After 1 h of equilibration, a sample of the liquid mixture was expanded into a trap, where the vacuum was previously done. The Precirol® collected was weighed and the dissolved CO_2 is measured via a manometer in the vacuum area. Each point was repeated twice.

At the same time, the solid/liquid/gas equilibrium line was measured using the first melting point method [19]. It consists in visualising the melting of a small quantity of Precirol® placed into a capillary. The capillary is inserted into a high-pressure cell equipped with sapphire windows. CO_2 is introduced at the pressure of interest and starts to dissolve inside the lipid. Then the temperature of the cell is slowly increased until the fat.

2.4. Determination of liquid and solid densities and molar volume of the fat

The molar volume can be calculated once the molecular weight and the liquid density are known. The molar weight was given by the supplier, 615 g/mol, and the liquid density was determined using a pycnometer. At 333 K, the liquid density was found to be 900 ± 40 kg/m^3. The solid density of Precirol® was measured using a helium pycnometer Accupyc 1330 (Micromeritics, USA) and was found to be 1000 ± 20 kg/m^3 (Table 3).

2.5. Estimation of viscosity of saturated Precirol® and interfacial tensile strength

Several physico-chemical parameters had to be determined to solve Eqs. (3), (6) and (7). The different parameters and experimental apparatus are gathered in Table 3.

The viscosity of melt Precirol® was measured using a RheoWin Pro 2.91 rheometer (ThermoHaake, Germany) at a temperature of 339.4 K and turned out to be 21.1×10^{-3} Pa s. The viscosity under supercritical conditions was estimated by referring to the literature [16]. This author showed that the viscosity of some vegetable oil mixtures (methyl oleate, castor oil) saturated by supercritical CO_2 follows a common behaviour. The viscosity of the fat can drastically decrease (divided by 9 when compared to the one at ambient pressure for castor oil at 16 MPa, 328 K and for a solubility of SC CO_2 of 20% w/w). Similarly, the assumption that the viscosity of melted Precirol® saturated by supercritical CO_2 before its expansion was 85% reduced, compared to the viscosity at atmospheric pressure, was done:

$$\eta(T) = \eta(T_{melt}) \times 0.15 \tag{9}$$

Thus, the viscosity of melted saturated Precirol® under supercritical conditions was estimated to be 3.17×10^{-3} Pa s. In addition, the evolution of the viscosity versus temperature was required. By measuring the viscosity of melted Precirol® versus temperature for a decreasing temperature from 343 K at atmospheric pressure we found an evolution like the one described by the Vogel–Fulcher rule [15]:

$$\eta(T) = \eta_o \exp\left(\frac{E_v}{k(T - T_d)}\right) \tag{10}$$

In (10), $\eta_0 = 14.08 \times 10^{-3}$ Pa s. T_d is the temperature at which the viscosity diverges, arbitrarily chosen to equal 223 K. This last value was considered as the lowest possible limit where CO_2 solidifies. E_v is the energy of activation for a viscous fluid: $E_v/k = 47.06$. All these parameters, except T_d, were based on a viscosity measurement performed between 343 and 315 K at atmospheric pressure.

Finally, the interfacial solid–liquid tensile strength was estimated by the Stefan–Skapski–Turnbull empiric law as shown in [15] and was found to be equal to 2.302×10^{-2} J/m^2:

$$\gamma_{SL} = K \frac{\Delta H_{melt}}{v_o^{2/3}} \tag{11}$$

In (11) K is a constant. This relation is generally applied to inorganic systems and K varies between 0.2 and 0.6. 0.2 was arbitrarily chosen in the present case. This relation implies that γ does not depend much on temperature. Neither empirical nor bibliographic evidence to document this were found.

3. Results and discussion

3.1. Solubility measurements and Precirol® melting point depression curve

Fig. 2 depicts the measured solubility of carbon dioxide in the lipid versus pressure at three different temperatures. The range of measured solubility varies from 0.23 g/g_{lipid} (333 K, 10 MPa) up to 0.37 g/g_{lipid} at 20 MPa and 323 K. The solubility of carbon

Table 3
Physico-chemical parameters for the study of the crystallization of Precirol®

Parameters	γ_{SL} (J/m^2)	$\eta(T)$ atmospheric pressure (Pa s)	$\eta(T)$ under supercritical conditions (Pa s)	Solid density (kg/m^3)	v_0 (m^3/molecule)
Determination	Stefan–Shapski–Turnbull	Rheometer	Hypothesis: $\eta(T) = \eta(T_{melt}) \times 0.15$	Helium pycnometer	Calculated with density
Values	23.02E−3	2.11E−2	3.17E−3	1000 ± 20	1.13E−27

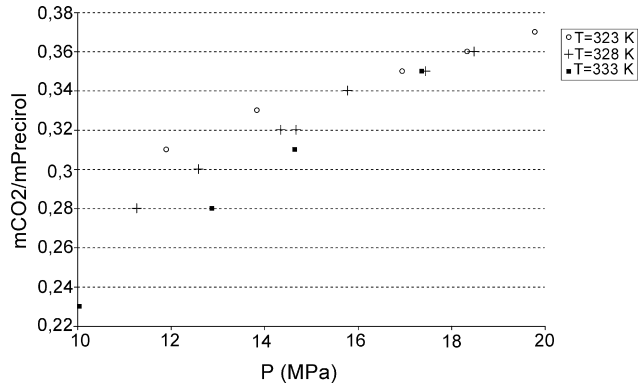

Fig. 2. Mass solubility of CO_2 onto Precirol® vs. pressure for three different temperatures tested.

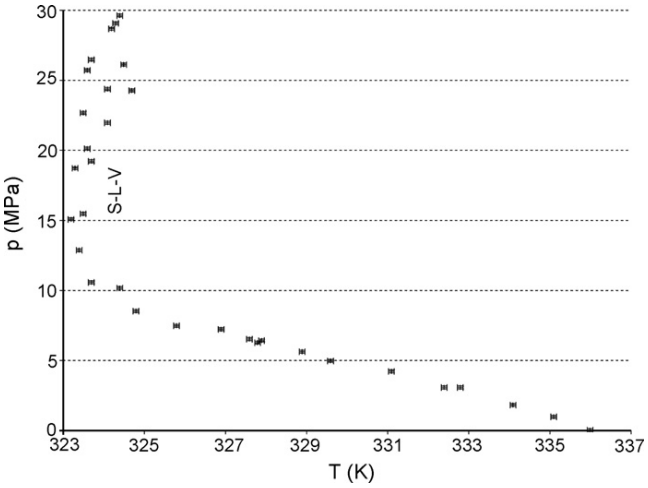

Fig. 3. Precirol® melting point evolution vs. pressure.

dioxide increases with pressure up to 17 MPa but diminishes with temperature. Above 17 MPa the solubility would be rather stable with pressure. The density of carbon dioxide decreases with temperature whereas the effect of temperature on vapour pressure is the opposite. Hence, the solubility of CO_2 in the heavy phase decreases with temperature.

The solid/liquid/gas equilibrium line is shown on Fig. 3. It appears that the melting temperature decreases with pressure up to a minimum of roughly 323 K and 11 MPa. This diminution is due to the dissolution of CO_2 into Precirol®. The melting temperatures are stabilized for intermediate pressures. For pressures above 30 MPa, the melting point increases again. The hydrodynamic pressure effect is dominant in this last case, and causes the restructuring of the solid and thus a raise in the melting point.

The S/L/G equilibrium curve was useful to locate the initial and final states when the mixture was expanded.

3.2. Heat capacities and measurement of the dissolution enthalpy of carbon dioxide into the fat

The calorimetry measurements done in the range 312–325 K, gave the solid heat capacity of Precirol®

$$c_{P,S}(T) = 1836.3 + 4.2427T - 3.9749 \times 10^{-3}T^2 \quad (\mathrm{J\,kg^{-1}\,K^{-1}}) \tag{12}$$

In the temperature from 337 up to 367 K, the following regression of liquid Precirol® heat capacity was found:

$$c_{P,L}(T) = 2263.8 - 6.1883T - 51.714 \times 10^{-3}T^2 \quad (\mathrm{J\,kg^{-1}\,K^{-1}}) \tag{13}$$

Both capacities were calculated at the normal Precirol® melting point, 330.1 K, for solid and liquid heat capacities (Table 2). Indeed, temperature had a weak effect on the capacities values. Concerning the determination of dissolution enthalpy, the heat flow difference between both trials gave the heat of dissolution of CO_2 into Precirol®. Two values were obtained 1.8 and 4.4 J/g as presented in the second column of Table 3. The precision of this measurement should be further investigated.

3.3. Solution of the thermodynamic balance with Matlab®

Eq. (2) was solved using Matlab® software. Among the numerous conditions of pressure and temperature before expansion, only two sets of initial condition are enough to cover the whole S/L/G phase diagram of Fig. 3. Indeed, when performing an expansion on a melted saturated compound, the system before expansion can be situated on the equilibrium line (case 1 of Table 4) or anywhere above the equilibrium curve (case 2 of Table 4). For temperatures below the equilibrium curve, the processed compound is not melted yet.

The physical state of Precirol® after expansion could be solid, liquid or a mixture solid/liquid. When considering that the final product was entirely melt ($f_L = 1$) or solid ($f_L = 0$), input parameters were temperature and pressure in the vessel T, P (Table 4), mass ratio of dissolved CO_2 to the total amount of CO_2 in the vessel, mass fraction of CO_2 in the system w_{CO_2}, mass ratio of melt Precirol® after expansion to the total weight of expanded fat f_L and the output parameter was the temperature after expansion T_F. When the final product was considered being a solid/liquid mixture, T_F was known, equal to T_{melt}, hence the output parameter was the liquid fraction expanded f_L.

Table 4
Numerical conditions entered within Matlab®

Input parameters	Pressure (MPa)	Temperature (K)	w_{CO_2}	f_L
Case 1	11.0	323	From 0 to 0.8	$f_L = 0, f_L = 1, 0 < f_L < 1$
Case 2	10.0	333	From 0 to 0.8	$f_L = 0, f_L = 1, 0 < f_L < 1$

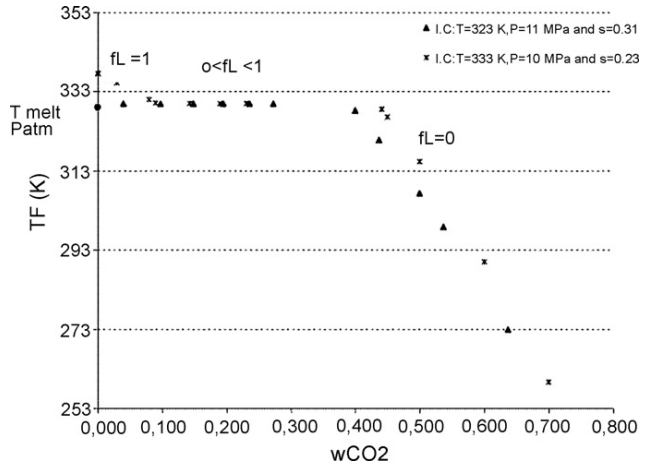

Fig. 4. Cases studied for the final temperature T_F reached after expansion of a Precirol® saturated solution.

Note that above $w_{CO_2} = 0.8$ the final temperatures calculated were below the sublimation point and the model could not be applied. However, the case when w_{CO_2} is between 0.8 and 1 is not very interesting on a process point of view because of unlikely operating conditions. The results of the computed Eq. (2) are summarised in Fig. 4.

Three cases are distinguished according to the three possible states of the expanded fat. Firstly, Precirol® was found to be entirely melted when T_F was higher than its melting point. Thus, fat was sprayed as droplets. In this case, the quantity of CO_2 dissolved in the fat and then expanded was lower than the quantity corresponding to the measured solubility value, that is to say after Fig. 2, for a mass fraction, w_{CO_2}, which was lower than 0.31 for case 1 and 0.23 for case 2 of Table 4. The first set of initial conditions tested (case 1 of Table 4), does not allow, in a thermodynamic point of view, Precirol® to be entirely liquid after expansion.

Secondly, if T_F was equal to the melting point, the fat was a mixture of melt and solid in equilibrium conditions. This result

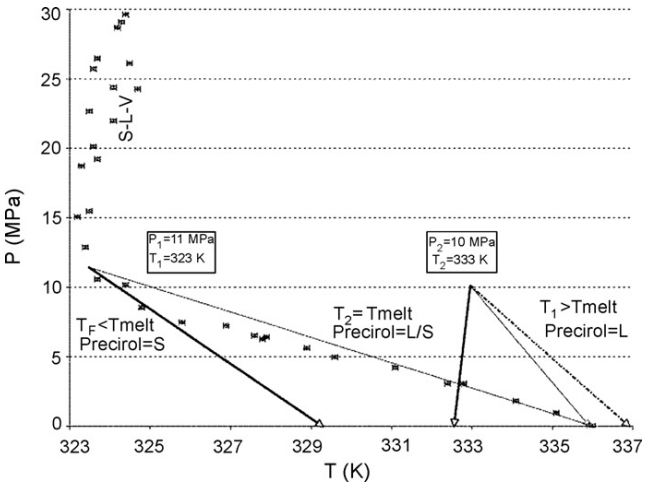

Fig. 5. Precirol® operating charts obtained for two different conditions before expansion.

was obtained when $0 < f_L < 1$. The model gave a final temperature equal to the melting point for quantities of CO_2 equal to or slightly under the solubility value, i.e. under 0.3.

Thirdly, expanded Precirol® was entirely solid when T_F was below the melting point. This happened for a high fraction of CO_2 expanded, higher than 0.4. The higher the quantity of CO_2, the lower T_F. In this last case, the exothermic effect released by Precirol® crystallization was not high enough to compensate the endothermic effect due to the expansion of CO_2.

These results allow for the setting up of "operating charts," as in [7]. The different cases studied appear in Fig. 5. These charts do not represent an operating path followed by the system but a thermodynamic link between initial and final states. They give information in order to anticipate the final state of the lipid after its expansion, versus the quantity of carbon dioxide expanded and when initial conditions in the vessel are known.

3.4. Comparison of the model with experimental study of PGSS expansion

To test the energy balance, the calculated T_F were compared with measured experimental ones. The experiments consisted in expanding the mixture Precirol®–CO_2 and varying the fraction of CO_2 in the mixture. The experimental case studied corresponded to case 1 of Table 4. A mechanical stirrer homogenized the mixture, and the temperature was measured just after expansion by a thermocouple TC SA, type K. After each expansion, Precirol® was collected and weighed. Then, knowing the initial amount of Precirol® placed into the vessel and the CO_2 solubility under these supercritical conditions, the quantity of CO_2 theoretically expanded and the corresponding final temperature, T_F, using Matlab® were calculated. The experimental results were in disagreement with the final temperature calculated with the energy balance as shown in Table 5.

Two possible explanations might be suggested. The first and main one is that the experimental mixture was not homogeneously mixed, meaning that a mixture containing mostly the heavy phase was first expanded. The recalculated w_{CO_2} corresponding to experimental T_F confirmed this. A remaining mixture containing mostly the light phase is expanded last. The second explanation is that the adiabaticity hypothesis does not hold.

Anyway, the energy balance was the first step needed in order to understand the process and to have an idea of the state and the temperature of the fat at the expansion outlet.

Table 5
Calculated final temperatures against experimental ones

Samples	w_{CO_2} calculated (g_{CO_2}/g mixture)	Experimental T_F (K)	Calculated T_F (K)
1	0.674	321.9	261.94
2	0.719	318	247.58
3	0.784	314.5	224.13
4	0.835	310.3	$T_F < T_{triple}$ CO_2—model is not valid

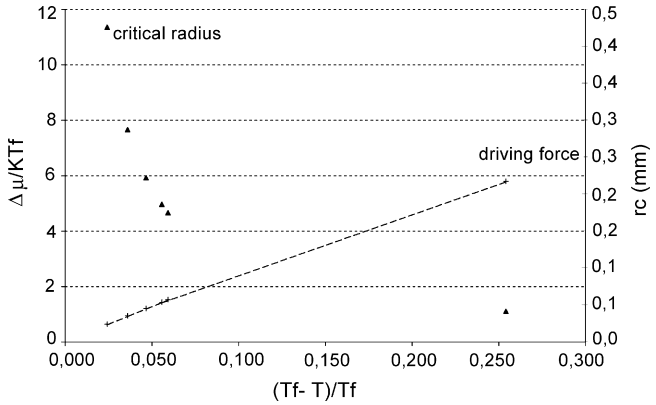

Fig. 6. Driving force associated with expansion of a supercritical saturated solution.

3.5. *Crystallization of the diglyceride by supercritical CO_2*

The second step was to investigate the kinetics of the crystallization of the fat. Only case 1 was studied (Table 4). Driving force values were calculated according to (3), considering only the first term. The results are gathered onto Fig. 6, considering dimensionless values. Note that the undercooling is turned into a dimensionless value using T_f, the fusion temperature. The difference between the driving force calculated with two terms and the one calculated with one term $(\Delta\mu_{1\text{term}} - \Delta\mu_{2\text{terms}})/\Delta\mu_{2\text{terms}}$, is of 0.5% for an outlet temperature of 243 K.

At the same time, the critical radius was also calculated (Fig. 6). As expected, the higher the driving force, the lower the critical radius.

Finally, the nucleation rate was also estimated, according to previous assumptions and measurements on the interfacial tensile strength and viscosity. Fig. 7 shows the nucleation rate given in entities per cm^3 of mixture and per second; it is shown that the rate quickly increases with undercooling and then the increase slows down and reaches a maximum according to classical melt crystallization [14]. At the low values of temperatures, undercooling may be so important that the viscosity of the solution may affect the mobility of the molecules. This maximum is then strongly dependent on viscosity values. Besides, values obtained for an interfacial tension of 23.02×10^{-3} J/m^2 are unrealistic, as shown in the following paragraph.

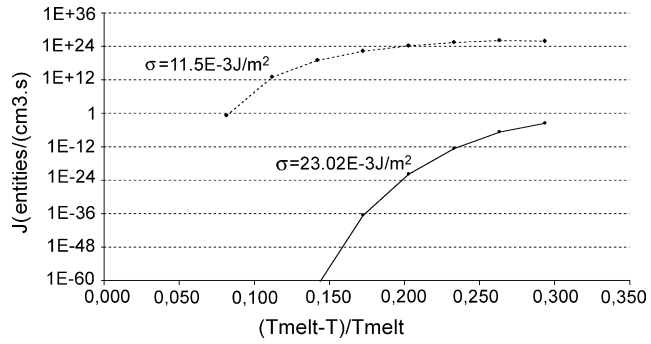

Fig. 7. Nucleation rate associated with the crystallization of Precirol®.

Table 6
Recrystallization temperature and heat of fusion of Precirol® in calorimetric experiments

Cooling rate (K/min)	$T_{\text{recrystallization}}$ (K)	Heat of fusion (J/g)
5	328.96	121 ± 4
10	328.55	115 ± 4
15	328.54	123 ± 4

Indeed, an order of magnitude of the characteristic values of crystallization time and final particle size can be estimated, supposing a value for the growth rate according to time $\equiv (JG^3)^{-1/4}$ size $\equiv (G/J)^{1/4}$ [20]. For γ_{SL} equal to 23.02×10^{-3} J/m^2 and a growth rate of $G = 3.10^{-7}$ m/s (this value of G was chosen according to results obtained by Kellens et al. [21] about isothermal crystallization of the β′-form of tripalmitin), characteristic values are out of a reasonable range irrespective of the undercooling. Conversely, for γ_{SL} equal to 11.5×10^{-3} J/m^2, a growth rate of $G = 3 \times 10^{-7}$ m/s, and an undercooling at 243 K, the characteristic time is about 1 s and the characteristic length is about 217 nm. These last values seem reasonable. Furthermore, some interfacial tensions of fat can be found in the literature: Ng, determined it for the β-polymorph of tripalmitin and found 9.45×10^{-3} J/m^2 [22]. Hence, 11.5×10^{-3} J/m^2 would be consistent with this last value. All these considerations confirm the drastic effect of the interfacial tension on the nucleation rate. Consequently, it is necessary to develop a way to measure it. In the literature, very few crystallization investigations in supercritical conditions can be found. Li and Matos have chosen an arbitrary value for the preexponential factor in (7), A_o/η, of 10^{39} nuclei/(m^3 s). It was deduced from the melted metals case [8]. Hence, it is difficult to evaluate its viability in the case of fats. Finally, in this study, Precirol® was assumed to be a pure compound, which is not the case. It is a mixture and there may be interactions between the major compound, a diglyceride and the other compounds. They might play the same role as impurities in crystallization and thus influence the nucleation and then the obtained polymorphism.

In order to test the influence of the cooling rate on the structure of the solid obtained, some calorimetric experiments were performed. Firstly the temperature was increased to melt the compound, then the temperature was decreased, so that the fat re-crystallized, and finally the temperature was increased a second time and the fat melted again. The cooling rate was varying and both the re-crystallization temperature and heat of fusion of the second heating were measured. Results are presented in Table 6 where it can be seen that the heat of fusion slightly varies with the cooling rate; as does the recrystallization temperature. One has to remember that the melting behaviour is determined, among other parameters, by the composition and by the polymorphs that are present [23,24]. It seems that the solid Precirol® obtained would remain roughly the same in terms of polymorphism (X-ray analysis would have to be done to confirm this) and the mixture of fats would not have been fractionated. In addition, similar experiments varying the cooling temperature between 263 and 233 K at a fixed cooling

rate of 5 K/min, were performed. They gave similar results (not shown here) that gave a roughly unchanged heat of fusion at the second heating. Hence, re-crystallized Precirol® seemed rather insensitive to a change in crystallization conditions.

4. Conclusions, further work

The thermodynamic balance of a supercritical fat solidification process was performed on the CO_2/Precirol® system. Fat solidification was obtained by expansion of a mixture of a CO_2 saturated melt fat and supercritical CO_2 in excess. It was then shown that the quantity of excess CO_2 that was expanded with the saturated liquid (or melt) allowed three physical states for the studied fat (solid, liquid or an equilibrium solid/liquid), according to the temperature and pressure conditions fixed before the expansion. The cases studied have enabled us to draw "operating charts" that give important information in order to implement the solidification process and to anticipate the temperature and the state of the expanded compound. The second point was an investigation of the crystallization aspect of such process. The melt media theory was considered to calculate the driving force, the critical radius and also the nucleation rates. Concerning the driving force, its approximation by the first term of the classic relation is precise enough. Nucleation rates calculated using an interfacial tension estimated using the Stefan–Skapski–Turnbull empiric law turned out to be unrealistic. By using an interfacial tension twice as small, 11.5×10^{-3} J/m^2, the nucleation rates become conceivable. The critical size and nucleation rates values must now be compared with classic melted media. The previous energy balance and the crystallization considerations are a first step towards a full modelling of such processes that also require hydrodynamic investigation.

Acknowledgements

Pierre Fabre Plantes et Industries (Gaillac, France) supported this work. Bernard Freiss from this company is especially thanked. Dr. Catarina Duarte and Raquel Sampaio de Sousa (ITQB, Portugal) are also gratefully acknowledged for their help with Precirol® solubility measurements. Sylvie Del Confetto and Severine Patry (ENSTIMAC, France) are also thanked for the experimental work they performed.

Appendix A. Peng–Robinson equation of state

Peng–Robinson equation of state (P.R. EoS) was obtained by improvement of the attractive pressure in the semi empirical van der Waals equation of state. The proposed equation is of the form:

$$P = \frac{RT}{v-b} - \frac{a(T)}{v(v+b)+b(v-b)} \tag{A.1}$$

In this equation, $a(T)$ is the attraction parameter and b the co volume according to van der Waals parameters.

According the authors, the molar enthalpy is described by:

$$H_\phi(T, P) = H^{\text{std}}(T) + Pv_\phi - RT + \frac{a - T\,(\mathrm{d}a/\mathrm{d}T)}{2\sqrt{2b}} \ln\left(\frac{v_\phi + (1-\sqrt{2})b}{v_\phi + (1-\sqrt{2})b}\right) \tag{A.2}$$

In this last equation, T the temperature, R the gas law constant, a the attraction parameter, b the co volume according to van der Waals and v_Φ is the molar volume chosen among the solutions of the cubic P.R. EoS to fit with the type of the phase Φ (the smallest value for liquid phase and the greatest value for vapour phase).

Appendix B. Neglect of kinetic energy

The variation of kinetic energy during the expansion step can be roughly estimated. Considering the hypothesis given in Section 1.1 of the present work, the global energy balance before and after the expansion can be given as:

$$\dot{m}_{\text{out}}\left(h_{\text{out}} + \frac{1}{2}u_{\text{out}}^2\right) - \dot{m}_{\text{in}}\left(h_{\text{in}} + \frac{1}{2}u_{\text{in}}^2\right) = 0 \tag{B.1}$$

h_{in}, u_{in} and h_{out}, u_{out} are, respectively, the enthalpies per unit mass and the velocities of the flows at the inlet and the outlet of the system. In steady state the mass flow rate of the CO_2/Precirol® mixture remained constant before and after the system. Velocities are linked to the cross section areas A_{in} and A_{out} and the densities ρ_{in} and ρ_{out} according to:

$$\dot{m} = \rho u A \tag{B.2}$$

By combination of the last two equations:

$$u_{\text{out}}^2 - u_{\text{in}}^2 = \dot{m}^2\left(\frac{1}{\rho_{\text{out}}^2 A_{\text{out}}^2} - \frac{1}{\rho_{\text{in}}^2 A_{\text{in}}^2}\right) \tag{B.3}$$

The densities of the mixture before and after expansion, respectively ρ_{in} and ρ_{out}, are linked to w_{CO_2}, the total mass fraction of the CO_2 in the mixture and supercritical CO_2 and to the densities of the pure compounds at the inlet and the outlet of the system according to following relations:

$$\frac{1}{\rho_{\text{in}}} = \frac{V_{\text{precirol}} + V_{CO_2}}{m_{\text{precirol}} + m_{CO_2}} = \frac{1}{m}\left(\frac{m_{\text{precirol}}}{\rho_{\text{precirol}}} + \frac{m_{CO_2}}{\rho_{CO_2}}\right) = \frac{1 - w_{CO_2}}{\rho_{\text{precirol}}(T_{\text{SC}}, P_{\text{SC}})} + \frac{w_{CO_2}}{\rho_{CO_2}(T_{\text{SC}}, P_{\text{SC}})} \tag{B.4}$$

$$\frac{1}{\rho_{\text{out}}} = \frac{1 - w_{CO_2}}{\rho_{\text{precirol}}(T_{\text{F}}, P_{\text{atm}})} + \frac{w_{CO_2}}{\rho_{CO_2}(T_{\text{F}}, P_{\text{atm}})} \tag{B.5}$$

Given that the aim is just to evaluate an order of magnitude of the variation of kinetic energy, any possible excess volume in the mixture was neglected.

$\dot{m}$, the mass flow rate of the CO_2/Precirol® mixture is the sum of the two components' flow rates:

$$\dot{m} = \dot{m}_{CO_2} + \dot{m}_{\text{precirol}} \tag{B.6}$$

Table 7
Parameters for the calculus of kinetic energy

Parameters	Values
$\dot{m}_{precirol}$(kg/s)	4.8E−3
$\dot{m}$(kg/s)	6.28E−3
r	0.31
A_{in} (m^2)	1.58E−5
A_{out} (m^2)	2.53E−4
$\rho_{CO_2 e}$(kg/m^3)	465.9
$\rho_{precirol_e}$(kg/m^3)	902.5
ρ_e (kg/m^3)	737.9
$\rho_{CO_{2s}}$(kg/m^3)	1.78
$\rho_{precirol_s}$(kg/m^3)	1000
ρ_s (kg/m^3)	7.55

The solubility of CO_2 into Precirol® is given by the ratio:

$$r = \frac{\dot{m}_{CO_2}}{\dot{m}_{\text{precirol}}} \tag{B.7}$$

Considering only the heavy phase, we can calculate $\dot{m}$ with the solubility:

$$\dot{m} = \dot{m}_{\text{precirol}}(1 + r) \tag{B.8}$$

The values for all the mentioned parameters are given in Table 7. Finally, the variation of kinetic energy is about 5.26 J/kg. This value is weak compared to the variation of the enthalpy of CO_2 linked to its expansion, which is about 8.9 kJ/g for an expansion from 11 MPa, 323 K to atmospheric pressure, 293 K.

Appendix C. Energy balance:

In the vessel upstream the system Σ, the light phase is supposed to be pure. A mass $m_{CO_2,\text{diss}}$ of CO_2 is dissolved in the melted Precirol®. At T_{SC}, P_{SC}, the enthalpy per unit mass h_{in} of the mixture is given by:

$$\begin{aligned}(m_{CO_2} + m_{\text{precirol}})h_{in} &= (m_{CO_2} - m_{CO_2,\text{diss}})h_{CO_2} \\ &\quad + m_{CO_2,\text{diss}}h_{CO_2,\text{diss}} + m_{\text{precirol}}h_{\text{precirol,L}}\end{aligned} \tag{C.1}$$

Let r be the solubility expressed in gram of dissolved CO_2 per gram of Precirol®, w_{CO_2} the mass fraction of CO_2, S the mass ratio of dissolved CO_2 compared to the total CO_2 in the autoclave:

$$S = r\frac{1 - w_{CO_2}}{w_{CO_2}} \tag{C.2}$$

and $\Delta h_{\text{diss}}(T, P)$ the dissolution enthalpy per unit mass of CO_2 onto Precirol® given by:

$$h_{CO_2,\text{diss}}(T_{SC}, P_{SC}) = h_{CO_2}(T_{SC}, P_{SC}) + \Delta h_{\text{diss}}(T_{SC}, P_{SC}) \tag{C.3}$$

Then:

$$\begin{aligned}h_{in} &= w_{CO_2}h_{CO_2}(T_{SC}, P_{SC}) + S\Delta h_{\text{diss}}(T_{SC}, P_{SC}) \\ &\quad + (1 - w_{CO_2})h_{\text{precirol,L}}(T_{SC}, P_{SC})\end{aligned} \tag{C.4}$$

The melted Precirol® is supposed to behave as an incompressible fluid with a constant specific volume v_L and a constant liquid heat capacity. At T_{SC}, P_{SC} its enthalpy can be written as:

$$\begin{aligned}h_{\text{precirol,L}}(T_{SC}, P_{SC}) &= h_{\text{precirol,L}}(T_{\text{melt}}, P_{\text{atm}}) + c_{P,L}(T_{SC}, T_{\text{melt}}) \\ &\quad + v_L(P_{SC} + P_{\text{atm}})\end{aligned} \tag{C.5}$$

Downstream the system, the CO_2 formed the vapour phase and Precirol® is partially solid. Let f_L the Precirol® mass ratio that remains liquid after expansion:

$$f_L = \frac{m_{\text{precirol,L}}}{m_{\text{precirol,L}} + m_{\text{precirol,S}}} \tag{C.6}$$

The enthalpy h_{out} of the mixture is given at T_F, P_{atm}, by:

$$\begin{aligned}h_{out} &= w_{CO_2}h_{CO_2,V}(T_F, P_{\text{atm}}) \\ &\quad + (1 - w_{CO_2})f_L h_{\text{precirol,L}}(T_F, P_{\text{atm}}) \\ &\quad + (1 - w_{CO_2})(1 - f_L)h_{\text{precirol,S}}(T_F, P_{\text{atm}})\end{aligned} \tag{C.7}$$

Introducing the crystallization enthalpy and the melting temperature of Precirol®:

$$\Delta h_{\text{crist}} = h_{\text{precirol,S}}(T_{\text{melt}}, P_{\text{atm}}) - h_{\text{precirol,L}}(T_{\text{melt}}, P_{\text{atm}}) \tag{C.8}$$

and by referring to the melting point of Precirol®:

$$h_{\text{precirol,S}}(T_F, P_{\text{atm}}) = h_{\text{precirol,L}}(T_{\text{melt}}, P_{\text{atm}}) + c_{P,L}(T_F - T_{\text{melt}}) \tag{C.9}$$

$$\begin{aligned}&h_{\text{precirol,S}}(T_F, P_{\text{atm}}) \\ &\quad = h_{\text{precirol,L}}(T_{\text{melt}}, P_{\text{atm}}) \\ &\qquad + \Delta h_{\text{crist}} + c_{P,S}(T_F - T_{\text{melt}})\end{aligned} \tag{C10}$$

Thus, introducing (C.4) and (C.5) and (C.7)–(C10), the final balance is:

$$\begin{aligned}&w_{CO_2}[h_{CO_2,V}(T_F, P_{\text{atm}}) - h_{CO_2,SC}(T_{SC}, P_{SC}) \\ &\quad - S\Delta h_{\text{diss}}(T_{SC}, P_{SC})] + \cdots(1 - w_{CO_2}[(1 - f_L)\Delta h_{\text{crist}} \\ &\quad - c_{P,L}(T_{SC}, T_{\text{melt}}) - (1 - f_L)(\Delta c_{P,\text{melt}})(T_F - T_{\text{melt}}) \\ &\quad - v_L(P_{SC} - P_{\text{atm}})] = 0\end{aligned} \tag{C.11}$$

References

[1] J.W. Tom, P.G. Debenedetti, Particle formation with supercritical fluids. A review, J. Aerosol Sci. 22 (1991) 555–584.

[2] E. Reverchon, R. Adami, Nanomaterials and supercritical fluids, J. Supercrit. Fluids 37 (2006) 1–22.

[3] E. Weidner, Z. Knez, Z. Novak, PGSS (particles from gas saturated solutions)—a new process for powder generation, in: G. Brunner, M. Perrut (Eds.), Proceedings of the 3rd International Symposium on Supercritical Fluids, Strasbourg, France, 1994, pp. 229–234.

[4] J.-J. Letourneau, S. Vigneau, P. Gonus, J. Fages, Micronized cocoa butter particles produced by a supercritical process, Chem. Eng. Process. 44 (2005) 201–207.
[5] A. Bertucco, G. Vetter, High Pressure Process Technology: Fundamentals and Applications, Industrial Chemistry Library, Elsevier Science, Amsterdam, 2001.
[6] Z. Knez, E. Weidner, Particles formation and particle design using supercritical fluids, Curr. Opin. Solid State Mater. Sci 7 (2003) 353–361.
[7] N. Elvassore, M. Flaibani, A. Bertucco, Thermodynamic analysis of micronization processes, Ind. Eng. Chem. Res. 42 (2003) 5924–5930.
[8] J. Li, H.A. Matos, E. Gomes de Azevedo, Two phases homogeneous model for particle formation from gas saturated solution processes, J. Supercrit. Fluids 32 (2004) 275–286.
[9] M. Rodrigues, N. Peiriço, H.A. Matos, E. Gomes de Azevedo, Modelling of particle formation from a gas-saturated solution process, in: G. Brunner, I. Kikic, M. Perrut (Eds.), Proceedings of the 6th International Symposium on Supercritical Fluids, Versailles, France, 2003.
[10] A.R. Sampaio de Sousa, M. Calderone, E. Rodier, J. Fages, C.M.M. Duarte, Solubility of carbon dioxide in three lipid-based biocarriers, J. Supercrit. Fluids 39 (2006) 13–19.
[11] D.Y. Peng, D.B. Robinson, A new two constants equation of state, Ind. Eng. Chem. Res. 15 (1976) 59–64.
[12] P. Ghosh, Review: prediction of vapour liquid phase equilibria using Peng–Robinson and Soave–Redlich–Kwong equation of state, Chem. Eng. Technol. 22 (1999) 379–399.
[13] R.C. Reid, J.M. Prausnitz, B.E. Poling, The Properties of Gases and Liquids, fourth ed., McGraw-Hill Book Company, New York, 1987.
[14] D. Kashchiev, Nucleation—Basic Theory with Applications, Butterworth Heinemann, Oxford, 2000.
[15] R.W. Hartel, Crystallization in Foods, Aspen Publishers, New York, 2001.
[16] E. Pomier, Etude d'un nouveau réacteur combinant enzymes, membrane et CO_2 supercritique, Application au biofaçonnement d'huiles végétales, these de doctorat de l'Université de Montpellier II, 2004.
[17] V. Jannin, E. Pochard, O. Chambin, Influence of poloxamers on the dissolution performance and stability of controlled-release formulations containing Precirol® ATO 5, Int. J. Pharm. 309 (2006) 6–15.
[18] W. Mehnert, K. Mader, Solid lipid nanoparticles: production, characterization and applications, Adv. Drug Deliver. Rev. 47 (2001) 165–196.
[19] E. Weidner, V. Wiesmet, Z. Knez, M. Skerget, Phase equilibrium (solid–liquid–gas) in polyethylenglycol carbon dioxide systems, J. Supercrit. Fluids 10 (1997) 139–147.
[20] J. Villermaux, R. David, Effet du micromélange sur la précipitation, J. Chim. Phys. 85 (1988) 273–279.
[21] M. Kellens, W. Meeussen, H. Reynaers, Study of the polymorphism and the crystallization kinetics of tripalmitin: a microscopic approach, J. Am. Oil Chem. Soc. 69 (1992) 906–911.
[22] W.L. Ng, Nucleation behaviour of tripalmitin from a triolein solution, J. Am. Oil Chem. Soc. 66 (1989) 1103–1106.
[23] A. Bell, M.H. Gordon, W. Jirasubkunakorn, K.W. Smith, Effects of composition on fat rheology and crystallisation, Food Chem. 101 (2007) 799–805.
[24] K.L. Humphrey, S.S. Narine, A comparison of lipid shortening functionality as a function of molecular ensemble and shear: crystallization and melting, Food Res. Int. 27 (2004) 11–27.